Environmental Science
Processes & Impacts

Accepted Manuscript

ROYAL SOCIETY OF CHEMISTRY

rsc.li/process-impacts

Environmental impact

Alumina (Al_2O_3) nanomaterials have potential uses in various industries and occupational exposure to Al_2O_3 dust may result in various damage among workers. Several *in vitro* and *in vivo* studies have shown the severe cytotoxicity, genotoxicity, oxidative stress and inflammation of neurocytes caused by Al_2O_3 nanoparticles. Presently, limited exposure data regarding airborne Al_2O_3 nanoparticles is obtained. This study monitored workplace exposure to airborne Al_2O_3 nanoparticles associated with separation and packaging processes in a pilot factory, which provides baseline data on workplace exposure to Al_2O_3 nanoparticles. These data can be used to inform standards for assessing workplace exposure to nanomaterials, or for further epidemiological studies on the health risks posed by Al_2O_3 nanomaterials.

Environmental Science: Processes & Impacts RSCPublishing

ARTICLE

Workplace Exposure to Airborne Alumina Nanoparticles associated with Separation and Packaging Processes in a Pilot Factory

Cite this: DOI: 10.1039/xoxxoooooox

Received ooth January 2012,
Accepted ooth January 2012

DOI: 10.1039/xoxxoooooox

www.rsc.org/

Mingluan Xing [a], Hua Zou [a], Xiangjing Gao [a], Bing Chang [b], Shichuan Tang [c]*, Meibian Zhang [a] **

Workplace exposure to airborne Al_2O_3 nanoparticles in a pilot factory was characterised by particle concentrations, size distribution, morphology and chemical composition, compared with background particles. Real-time variations in number concentration ($NC_{20–1000nm}$), respirable mass concentration ($MC_{100–1000nm}$), active surface area concentration ($SAC_{10–1000nm}$) and particle size were measured at production locations involved in separation and packaging activities. Measurements during stable production periods showed significant increases in the various concentrations of agglomerated Al_2O_3 nanoparticles (about 305 nm) at separation locations, compared to those of background particles ($p < 0.01$). The size distribution model for separation processes might switch to primary nanoparticles (21–26 nm) during periods of unstable production. Packaging activities also caused significant increases in different concentrations of Al_2O_3 nanoparticles (about 90 nm) compared to background particles ($p < 0.01$). These particles exhibited a bimodal size distribution and floccus or cloudy-like agglomerates of primary nanoparticles. $NC_{20–1000nm}$ and active $SAC_{10–1000nm}$ variations showed the same trend, and were temporally consistent with particle emission scenarios or worker activities, but differed from that for respirable $MC_{100–1000nm}$. There was strong correlation between active $SAC_{10–1000nm}$ and $NC_{20–1000nm}$ ($r = 0.823$), moderate correlation between active $SAC_{10–1000nm}$ and respirable $MC_{100–1000nm}$ ($r = 0.666$) and relatively weak correlation between $NC_{20–1000nm}$ and respirable $MC_{100–1000nm}$ ($r = 0.361$). These findings from the pilot factory suggest significant exposure to Al_2O_3 nanoparticles or their agglomerates, associated with separation and packaging processes. The number and active surface area concentrations may be distinct from mass concentration and might be more appropriate for characterizing exposure to airborne nanoparticles

Highlighting: Workplace exposure to airborne alumina nanoparticles associated with separation and packaging Processes

Introduction

Alumina (Al_2O_3) nanomaterials have potential uses in various industries, such as high-performance paints, abrasives, flooring material, ultrafiltration membranes, jet fuel, rocket propulsion fuel, heat-enhancing nano fluids and vaccines.[1–8] These wide applications, and their unique properties such as small size, high surface area and high surface reactivity, have given rise to concerns regarding the uncertainty of their potential health risks.[9] It is well known that occupational exposure to Al_2O_3 dust may result in nervous system damage among workers. Several *in vitro* and *in vivo* studies on Al_2O_3 nanoparticles found much more severe cytotoxicity, genotoxicity, oxidative stress and inflammation of neurocytes, as well as nervous system damage, compared with their counterpart materials of microscale size or relatively inert nano carbon.[10–15] These findings suggest that some nanoparticle characteristics, such as particle size, chemical composition, and concentration, play important roles in the potential negative health effects induced by Al_2O_3 nanoparticles.

Experimental studies, as the main research approach for assessing the health risks of nanoparticles, need to be verified by epidemiological studies or field exposure investigations. Presently, limited exposure data regarding airborne Al_2O_3 nanoparticles is obtained, mainly from two approaches: air

monitoring in real workplaces, and process-based studies in simulated workplaces. Kuhlbusch et al.[16] investigated workplace exposure to TiO_2 and Al_2O_3 nanoparticles, and observed no significant release of particles < 100 nm in wet and combustion-based production processes; however, when a bag was overfilled, a release of agglomerates > 400 nm was observed. Methner et al.[17] found a significant release of Al_2O_3 nanoparticles (50–80 nm) from the radio-frequency induction plasma reactor in a research and development laboratory. In a simulated industry workplace , Tsai et al.[18,19] reported a significant release of Al_2O_3 nanoparticles during the compounding process of nanocomposite with nanoscale alumina. The authors[20,21] also investigated the protective effects of different laboratory fume hoods on nanoalumina and nanosilver, and found that the handling of dry, nano-scale powders inside laboratory fume hoods can result in significant release of airborne nanoparticles to the laboratory environment. This release is affected by many variables such as hood design, hood operation, work practices, etc. In research laboratories, Demou et al[22] reported significant particle emission and exposure during the synthesis of nanoalumina composites.

Our study attempts to address the scarcity of data from real workplaces on the exposure to airborne Al_2O_3 nanoparticles. We monitored workplace exposure to airborne Al_2O_3 nanoparticles associated with separation and packaging processes in a pilot factory in Jiangsu Province, East China. In detail, we investigated the characteristics of Al_2O_3 nanoparticles (including total particle concentration, size distribution, morphology, chemical composition and accumulative percentage of nanoparticles by number and mass) compared with background particles, as well as temporal variations in total particle concentrations and particle sizes associated with particle emission or worker activities. Relationships between different real-time particle concentrations such as number concentration (NC), active surface area concentration (SAC) and respirable mass concentration (MC) were also analysed because of the uncertainty as to the most appropriate exposure metric for nanoparticles

Methods

Description of workplace

Two neighbouring workshops (namely, production and packaging) manufacturing γ-Al_2O_3 nanomaterials in a pilot factory in Jiangsu Province of East China were selected for the field investigation. Fig. 1 (a) illustrates the production workshop, which is next to the packaging workshop (Fig. 1 (b)). The production workshop consists of four areas, i.e. crushing area, reactor area, HCl recovery area and control room. The packaging workshop comprises packaging area, air compressor area, the part-stacking area and end-product storage area. In this plant, γ-Al_2O_3 nanomaterials were produced using the gas-phase method. The production process is summarised as follows: (1) grinding: large-size $AlCl_3$ particles are ground to smaller sizes in an enclosed container; (2) chemical reaction: the $AlCl_3$ particles are fed into a reactor with air and nitrogen. The Al_2O_3 nanomaterials are produced using gas-phase method in the reactor; (3) separation: the Al_2O_3 nanoparticles are separated from air using the technique of air back-flushing in a separator; (4) packaging: the Al_2O_3 nanomaterials are transported to a packaging workshop by pipeline for automatic packaging. Two processes, namely, separation and packaging, have the potential to generate airborne nanoparticles (Table 1), and so their corresponding locations within the facility were selected as the sampling sites. The production status was sometimes unstable, because the pilot factory was in the trial phase of production, during which there was frequently visible emission of particles. Hence, particle release at the separation location was compared for two kinds of production status: stable and unstable. Meanwhile, outdoor background particles were used as the control (Fig. 1). No ethical statement was prepared to accompany the field study, since no human participants were recruited. The study was approved by the Zhejiang Provincial Center for Disease Control and Prevention, China.

Monitoring and sampling system

Table 2 shows the monitoring and sampling system. The real-time system monitored total particle concentrations (number, mass and surface area) and the size distribution by number. The membrane-based sampling system was used to collect airborne nanoparticles to analyse their mass morphology, elemental composition and the size distribution by mass.

The total number concentrations were determined using a P-Trak ultrafine particle counter (Model 8525, TSI, USA), which is a portable condensation particle counter (CPC). The counter was calibrated by the manufacturer and was set to zero each day, prior to sampling. The isopropyl alcohol cartridge was replaced every 5.5 h. The respirable mass concentrations were measured using a real-time aerosol monitor (DustTrak 8530, TSI, USA), which is a portable laser-scattering photometer. The monitor was calibrated by the manufacturer. Before sampling, a monitor reading of zero was confirmed using a high-efficiency particulate absorption (HEPA) filter. The active surface area concentration (SAC) was determined using a surface area monitor (Aero TrakTM 9000, TSI, USA). The monitor, which consists of a diffusion charger and an electrometer, was used in the alveolar deposition mode. The size distribution by number of the nanoparticles was determined using a scanning mobility particle sizer (SMPS, Model 3034, TSI, USA). The SMPS contains a differential mobility analyser (DMA) and a CPC that can determine the particle size distribution by number of nanoparticles based on their electrical-mobility diameters. The instrument was calibrated by the manufacturer. Several size parameters, including the mode (i.e., the size corresponding to the peak concentration), arithmetic mean and geometric mean, were derived from the SMPS data. The estimated SAC was calculated with SMPS software (Aerosol Instrument manager) by assuming a spherical geometry for Al_2O_3 nanoparticles.[23]

The morphologies and elemental compositions of nanoparticles were analysed using scanning electron microscopy (SEM, S4800, HITACHI, Japan) and energy-dispersive X-ray spectroscopy (EDX, S4800, HITACHI, Japan), respectively. Airborne nanoparticles were collected using a cascade impactor (Nano-MOUDI, 125A, MSP, USA). The impactor comprised 13 stages, corresponding to cut sizes of 10000, 5600, 3200, 1800, 1000, 560, 320, 180, 100, 56, 32, 18, and 10 nm. The morphology and elemental composition of the Al_2O_3 nanoparticles collected at the 13th stage (i.e., those with a cut size of 10 nm) were analysed. In this study, the accumulative percentage by mass (APM) of nanoparticles (less than 100 nm) in the total mass concentration (less than 560 nm) was calculated. For comparison, the accumulative percentage by number (APN) of nanoparticles in the total number concentration (less than 469.8 nm) was also calculated from SPMS data. Thus, the two kinds of accumulative percentages (by number and by mass) could be compared to evaluate whether the number or mass of nanoparticles was predominant.

Sampling or testing strategy

The sampling process, which was performed in September 2012. Three-time 3 days measurements were performed for the separation and packaging processes under the stable production status in order to avoid the time variations and capturer the real exposures for workers. During the different sampling days, manufacturing parameters, volume of production, worker tasks and engineering control measures were the same under the stable production status. Table 1 shows day 2 was a representative among the three-day sampling period. In addition, only one-time 1 day measurement (i.e. day 1 in Table 1) was performed for the separation process under the unstable production status that occurred at a very low-frequency. The one-time monitoring results could be a supplement for the real exposure for workers. After gathering general information related to the product and its manufacture, an observational walkthrough survey was conducted using the CPC, to identify potential sources of particle emission. The sampling protocol was as follows: (1) activity-based measurements: the sampling locations were selected on the basis of the information gathered and the walkthrough survey, while also considering several other factors such as the air movement and currents, the work tasks and whether they would allow for the placement of large instruments without hindering normal work activities. The sampling locations are shown in Fig. 1. Activity-based measurements were performed before and during work. Sampling was performed 1.3 m above the floor and close to the breathing zone of the workers potentially exposed to the Al_2O_3 nanoparticles. The sampling period covered a complete dayshift of the workers; (2) background measurements: outdoor atmospheric particles were sampled to establish background levels. No incidental particle sources were present in the production workshop during the sampling period. However, some worker activities in the packaging workshop that were unrelated to the packaging activity (e.g., transporting containers of liquid nitrogen) were observed during the sampling period. The timeline of the test protocol is briefly listed in Table 1. Some key events that might affect particle concentrations are listed in Table 5.

Statistical analysis

One-way analysis of variance (ANOVA), followed by the Dunnett's T3 multiple comparison method, was used to analyse the differences in the total particle concentrations corresponding to the different sampling locations and backgrounds. Pearson correlation was applied to analyse the relationships between different exposure metrics.

Results and discussion

Particle characteristics

The characteristics of Al_2O_3 nanoparticles at the separation and packaging locations are listed in Table 3. The $NC_{20–1000nm}$, respirable $MC_{100–1000nm}$, active $SAC_{10–1000nm}$ and estimated $SAC_{10–487nm}$ at separation (under stable or unstable production status) and packaging locations were significantly higher than corresponding background levels sampled outdoors ($p < 0.01$). Table 3 also shows the concentration ratios at the background and sampling locations for $NC_{20–1000nm}$, respirable $MC_{100–1000nm}$, active $SAC_{10–1000nm}$ and estimated $SAC_{10–487nm}$. For instance, the concentration ratio in $NC_{20–1000nm}$ ranged from 1.79 to 4.94. These results suggest that the separation and packaging processes conducted in real workplaces are able to generate high levels of nanoparticles. The above four particle concentrations at separation locations were significantly higher during unstable production status than during stable production ($p < 0.01$). The estimated SAC calculated from SMPS data was much higher than the active SAC, which was measured by the Aero TrakTM 9000 ($p < 0.01$). The estimated SAC reflects total surface area of particles suspended in air, whereas the Aero TrakTM 9000 monitor indicates the surface area of the fraction of these particles that deposit in either the tracheobronchial or alveolar regions of the human respiratory tract.

Airborne nanoparticles showed bimodal size distribution, with different mode sizes between the separation (in stable or unstable production status) and packaging processes (Table 3). Moreover, these shapes of bimodal size distribution differed from that (unimodal) for outdoor background samples, which suggested that the particles found at the highest concentration in the air of the workshop differed from outdoor background particles. The finding of bimodal size distribution of airborne nanoparticles in this study is in agreement with other field studies,[24] where bimodal size distributions (often with size modes around 200–400 nm and 1000–20,000 nm) were observed during end-product production activities such as bagging and reactor cleaning. However, the modes varied substantially between studies. In some cases, the mode of the size distribution was within the nano range.[19,25]

Fig. 2 (a) and (b) show the floccus agglomerates of Al_2O_3 nanoparticles collected from separation process. Fig. 2(c) shows cloudy-like agglomerates of Al_2O_3 nanoparticles collected from packaging process. These particle shapes were significantly different from that (irregular) of outdoor background samples. Table 4 lists the chemical compositions of particles sampled in both the indoor workplace and outdoor background locations. It is clear that oxygen (O) and aluminium (Al) were the predominant elements in the particles collected from the separation and packaging locations, which were significantly different from those of background particles. In general, these results for real-time particle concentrations (NC, SAC and MC), size distribution and SEM analysis further confirm that separation processes during stable production could result in significant workplace exposure to agglomerated Al_2O_3 nanoparticles with mode size approximately 305 nm; separation processes during unstable production could lead to significant leakage of primary Al_2O_3 nanoparticles with mode size of 21–26 nm; and packaging processes are associated with the release of high levels of Al_2O_3 nanoparticles with mode size approximately 90 nm.

At present, there is limited data available on exposure to Al_2O_3 nanoparticles in real workplaces or laboratories. A previous study reported that wet and combustion-based production processes did not release Al_2O_3 nanoparticles, but that bagging processes could sometimes result in significant release of particle agglomerates larger than 400 nm,[16] which supports our finding that packaging processes could lead to particle emission. Methner et al[17] examined a radio-frequency induction plasma reactor in a research and development laboratory, and found that the $NC_{10–1000nm}$ fraction of Al_2O_3 nanoparticles (50–80 nm) could reach 6700–15580 particles/cm^3, compared with background level of 2700 particles/cm^3. This was attributed to cleaning operations (brush-down of plasma torch, filter chamber and cyclone). The authors reported concentration ratio of cleaning activity and background level is from 2.48 to 5.77, which is similar to that (2.26–4.94) of separation process observed in our study. Tsai et al.[19] reported more than twofold increase in $NC_{5.6–560nm}$ for nanoparticles (45 or 190 nm) from background level, caused by the process of compounding a nanocomposite using nanoalumina as fillers. These released nanoparticles might be a complex mixture of individual nanoalumina particles, agglomerates of those particles and polymer fume particles through STEM analysis. Tsai et al[20] also reported that the handling of dry powders consisting of Al_2O_3 nanoparticles inside laboratory fume hoods could result in significant release of airborne nanoparticles from the fume hood to the laboratory environment and the researcher's breathing zone; the release was affected by many variables, including hood design, hood operation, and working practices. Demou et al.[22] investigated particle emission and exposure during synthesis of nanoalumina composites (Pt/Ba/Al_2O_3) in a research laboratory, and found that levels of $NC_{10–1000nm}$ nanoparticles were 3.14–16.83 times greater than that of background particles. The concentration ratio reported for synthesis and background locations was higher than that (2.26–4.94) of the separation process observed in our study. Compared to other airborne nanoparticles (e.g. carbon nanotube and metal-based nanoparticles) in workplaces or laboratories, the concentration ratios of $NC_{10–1000nm}$ during production activities varied from 1.0 to 6.94.[26–28]

Variations in total particle concentrations

The temporal variations in the total particle concentrations at the separation location are shown in Fig. 3 and Fig. 4. Fig.3 (a) illustrates that $NC_{20–1000nm}$ fluctuated sharply, with maximum concentration (4.96×10^5particles/cm^3) approaching the maximum detection limit of the CPC under unstable production status, due to frequent back-flushing by high-pressure air during the separation process (Table 5). In such a high concentration environment (>2.0×10^5 particles/cm^3), the P-Trak particle counter may underreport nanoparticle number concentrations due to coincidence errors, i.e. more than one particle can pass through the sensing region at a time, with these then counted as a single particle.[29,30] Although NC at various work sites under stable production status in this study was less than 2.0×10^5 particles/cm^3, these coincidence errors should be noted. Similarly to $NC_{20–1000nm,}$ distinct temporal variation was also observed for active $SAC_{10–1000nm.}$ During stable production, $NC_{20–1000nm}$ and active $SAC_{10–1000nm}$ showed the same trend, especially at the time of incidental back-flushing by compressed air. In contrast, the temporal variation in respirable $MC_{100–1000nm}$ was quite different from those of $NC_{20–1000nm}$ and active $SAC_{10–1000nm}$ and was not consistent with the occurrence of key events during either unstable or stable production (Fig.4 (a) and (b)). Hence, it is clear that the variations in $NC_{20–1000nm}$ and active $SAC_{10–1000nm}$ were associated with unreasonable process design in the separator, i.e. too frequent back-flushing via excessively high air pressure, leading to significant particle leakage from the cold-air inlet.

Fig. 5 (a) and Table 5 show that the variations in $NC_{20–1000nm}$ and active $SAC_{10–1000nm}$ were significantly affected by two kinds of worker activities: collection for nanomaterial end-product (related to nanomaterials) and indoor transportation (not related to nanomaterials). $NC_{20–1000nm}$ and active $SAC_{10–1000nm}$ concentrations had been significantly higher than that of outdoor background ($p < 0.01$) since the packaging device became operational. When workers were transporting liquid nitrogen containers and opening the workshop door (time of occurrence 9:44–9:50 hr), which readily led to the re-entrainment of dust from the floor, The $NC_{20–1000nm}$ and active $SAC_{10–1000nm}$ increased dramatically and then declined gradually. Their increasing speed was much faster than that of respirable $MC_{100–1000nm}$ at the time of 9:44–9:50 hr (Fig. 5 (b)). End-product collection activity at 10:26–10:29 and 11:12–11:15 resulted in a sudden increase in $NC_{20–1000nm}$, active $SAC_{10–1000nm}$ and respirable $MC_{100–1000nm}$. Similarly, the extent of change in $NC_{20–1000nm}$ and active $SAC_{10–1000nm}$ was greater than that of respirable $MC_{100–1000nm}$, especially during the second packaging activity. These results suggested that respirable $MC_{100–1000nm}$ in this study was less sensitive to levels of exposure to nanoparticles than were $NC_{20–1000nm}$ or active

$SAC_{10–1000nm}$. This finding is supported by our previous study, which demonstrated that respirable mass concentration was not as sensitive as number concentration or surface concentration in measuring nanoparticle levels at different welding points, sampling distances, and background particles at an automobile manufacturing facility.[31]

Furthermore, increased concentrations of airborne Al_2O_3 nanoparticles (about 90 nm, determined by SMPS) were clearly associated with packaging activities. Besides the worker activities, the particle size is a critical factor in theory that affecting active SAC. Active SAC is defined as the surface of a particle that is involved in interactions with surrounding gas. It is equivalent to the geometric surface area for spherical particles, and proportional to particle diameter squared when particle diameter is much smaller than the mean free path of surrounding gas. However, this equivalence no longer holds when particle sizes increase and active surface area of a particle increases proportionally to particle diameter.[32,33] In addition, respirable MC is determined using an aerosol photometer (DustTrak) based upon light scattering, which is also strongly affected by the particle size. Particles smaller than about 50 nm do not interact strongly with electromagnetic radiation at optical or near optical wavelengths, and so are not detected efficiently by light blocking or scattering.[34]

There is an interesting phenomenon that the bimodal size distribution (with 99.70 nm mode size of first peak and 23.11 nm of second peak) of re-entrained dust from the workshop floor, which was caused by indoor transportation, was quite similar to that for packaging activity. This finding suggests that the floor dust results from long-term sedimentation of airborne Al_2O_3 nanoparticles that were previously released but not promptly cleaned. Some field studies reported that an increase in nanoparticle concentrations was often associated with particle sources other than the nanomaterial-related activities or emissions, including vacuum pumps, diesel-powered fork lift trucks, or other combustion or heat-generating activities such as welding, soldering, or heat-sealing. [18,24,25,35]

Variations in particle size

Fig. 6 shows the temporal variations in particle sizes, that is, in their mode, arithmetic mean and geometric mean. The change in arithmetic mean and geometric mean sizes was similar, but less sensitive than that for modal size. It is clear that nanoparticles released from the separation process showed two particle size modes, i.e. agglomerated (about 305 nm) and primary (21–26 nm). Table 5 and Fig. 6 (a) show that the agglomerate of nanoparticles (about 305 nm) predominated as a result of particle spraying from a cold-air inlet, and that primary nanoparticles (about 26 nm) predominated in scenarios of much greater particle leakage. Fig. 6 (b) illustrates that the increase in primary particle size from 26 nm to 148 nm coincided with a 6-minute maintenance activity for liquid nitrogen containers, which might result in re-entrainment of dust from the workshop floor. The size distributions at the separation and packaging locations were relatively steady, which differs from a previous experimental study on airborne nanoalumina or nanosilver exposure while using different fume hoods.[21] The authors reported that exposure to airborne nanoparticles within the hood operator's breathing zone covered the size range 5–20 mm, and the size distribution pattern of the particles from the constant-volume hood varied with face velocity, i.e. very few particles of any size were released at a face velocity of 0.4 m s^{-1}; particles of 20 nm diameter predominated at 0.6 m s^{-1}; and particles of 200 nm diameter were released at 1.0 m s^{-1}.

Relationships among $NC_{20–1000nm}$, $SAC_{10–1000nm}$ and $MC_{100–1000nm}$ Table 3 shows that the APNs of airborne nanoparticles at different locations ranged from 43% to 73%, which was significantly higher than the corresponding APMs of 20% to 25%. The ratios of APN to APM ranged from 2.18 to 3.39. These results indicate that the number concentration of airborne nanoparticles was predominant in total number concentration, whereas the mass concentration accounted for only a small fraction of the total mass concentration. This result was supported by our previous study, in which welding nanoparticles by number comprised 60.7% of particles, whereas measurement by mass accounted for only 18.2% of the total particles.[31] Mass concentration, which is the metric used traditionally for assessing exposure to aerosols, may be inadequate for characterising exposure to nanoparticles, because nanoparticles usually account for only a small fraction of the total mass concentration.[36–38]

Table 6 shows a strong correlation between $NC_{20–1000nm}$ and active $SAC_{10–1000nm}$ (r = 0.823), moderate correlation between active $SAC_{10–1000nm}$ and respirable $MC_{100–1000nm}$ (r = 0.666) and relatively weak correlation between $NC_{20–1000nm}$ and respirable $MC_{100–1000nm}$ (r = 0.361). The major reason for the correlation between the three exposure metrics from poor to strong is dependent on the particle size and size-dependent fraction. The high correlation found between NC and active SAC could be related to the fact that the SMPS and AeroTrak both count numbers of particles, with the AeroTrak then transforming the number of particles into surface area.

The possible association between the number and mass concentrations has been explored in several field studies using real-time measurements. No correlation between particle number concentration and mass concentration was found during clean-up activities associated with the production of carbon black.[39] Yeganeh et al.[40] reported a weak correlation between the particle number concentrations (up to 650 nm) and the mass concentration (PM2.5) corresponding to activities related to the processing of fullerenes. Demou et al.[27] observed a correlation between the mass (PM1.0) and number (up to 1.0 μm) concentrations in a facility for producing metal-based nanomaterials only during a few days of a 17-day measurement period. Data on the correlation between SAC and NC or MC is limited in the case of engineered nanoparticles, and the available information on these relationships is usually obtained from studies of non-engineered nanoparticles. It has been reported that there is a strong correlation between SAC and NC,

and a relatively weak correlation between SAC and MC.[31,37] Many toxicological studies have demonstrated that the unique characteristics of nanoparticles, such as large surface area and higher particle number per unit mass, are associated with more pronounced inflammatory response or greater oxidative stress in the lungs.[41–46] These findings suggest that MC, as a traditional metric for aerosol exposure, may be inadequate in characterising nanoparticle exposure, and that NC and SAC are much more relevant as metrics for characterising exposure to Al_2O_3 nanoparticles.

Conclusions

Separation processes during stable production could result in significant emission of agglomerated Al_2O_3 nanoparticles with estimated mode size of 305 nm. The size distribution model might switch to primary nanoparticles with modal size 21–26 nm during periods of unstable production. Packaging processes also resulted in increased concentrations of Al_2O_3 nanoparticles (mode size of about 90 nm). These particles exhibited a bimodal size distribution and floccus or cloudy-like agglomerates of primary nanoparticles. The variations in $NC_{20–1000nm}$ and $SAC_{10–1000nm}$ were the same and were associated with particle emission scenarios or the occurrence of nanomaterial-related activities, but differed from that for respirable $MC_{100–1000nm}$. There was a high degree of correlation between active $SAC_{10–1000nm}$ and $NC_{20–1000nm}$, moderate correlation between active $SAC_{10–1000nm}$ and respirable $MC_{100–1000nm}$, and relatively low degree of correlation between $NC_{20–1000nm}$ and respirable $MC_{100–1000nm}$. NC and active SAC metrics may be distinct from MC and might be more appropriate for characterizing exposure to airborne nanoparticles.

This study provides baseline data on workplace exposure to Al_2O_3 nanoparticles. These data can be used to inform standards for assessing workplace exposure to nanomaterials, or for further epidemiological studies on the health risks posed by Al_2O_3 nanomaterials. The number and surface-area concentrations might be much more appropriate than the mass concentration when selecting exposure metrics to characterise nanoparticle exposure or assess the dose–effect relationship of nanoparticles in workplaces. Comparisons of the particle characteristics (concentration, size distribution, morphology and chemical composition) corresponding to the airborne nanoparticles and the background particles must be considered in the absence of an occupational exposure limit for nanoparticles. To better understand the exposure characteristics of airborne nanoparticles, it is necessary to identify the nature of nanoparticles, the dynamic changes in their metric-dependent concentrations and the variations in their size and size distribution during manufacturing, handling and end-use processes. In addition, it is important to exclude the effect of other particle sources or non-nanomaterial-related activities when assessing workplace exposure to engineered nanoparticles. Finally, better process design with appropriate air pressure for back-flushing to separate the Al_2O_3 nanomaterials is critical to reducing particle emission from the cold-air inlet. However, a few limitations of the study should be pointed out. The exposure data were obtained using static measurements, and thus should be interpreted with care as estimates of personal exposure. Additionally, the exposure characteristics regarding concentration, size distribution and chemical composition, as well as the appropriateness of different exposure metrics for nanoparticles need to be further verified by epidemiological studies.

Acknowledgements

This work was supported by the Natural Science Foundation of China (81472961); the Health Standards Fund of the Ministry of Health, China (20130215); the Co-constructed Projects by the National Health and Family Planning Commission of China and the Health Bureau of Zhejiang Province (No. WKJ2014-ZJ-0); the Science and Technology Fund of the Health Bureau of Zhejiang Province, China (Nos. 2014KYB061, 2012KYB050 and 201482330); the Innovation Projects of the Beijing Academy of Science and Technology （PXM2014-178304-000001-00130138）and the Innovation Teamwork Projects of the Beijing Academy of Science and Technology (G201402N).

Notes and references

[a] Zhejiang Provincial Center for Disease Control and Prevention, Hangzhou 310051, Zhejiang, People's Republic of China.
[b] China National Institute of Occupational Health and Poison Control, Beijing 100050, People's Republic of China.
[c] Beijing Municipal Institute of Labor Protection, Beijing 100054, People's Republic of China

** Corresponding author. E-mail: mbzhang@cdc.zj.cn
*Corresponding author. E-mail: tsc3496@sina.com

1 W. G. Sawyer, K. D. Freudenberg, P. Bhimaraj and L. S. Schadler, *Wear*, 2003, **254**, 573–580.
2 V. Landry, B. Riedl and P. Blanchet, *Prog. Org. Coat.*, 2008, **61**, 76–82.
3 A. S. Khanna, *Asian J. Exp. Sci.*, 2008, **21**, 25–32.
4 K. A. DeFriend, M .R. Wiesner and A. R. Barron, *J. Membr. Sci.,* 2003, **224**, 11–28.
5 W. K. Lewis, B. A. Harruff, J. R. Gord, A. T. Rosenberger, T. M. Sexton, E. A. Guliants and C. E. Bunker, *J. Phys. Chem. C*, 2010, **115**, 70–77.
6 L. Luca, L. Galfetti, F. Severini, L, Meda, G. Marra, A. Vorozhtsov, V. Sedoi and V. Babuk, *Combust Explo Shock+*, 2005, **41**, 680–692.
7 K. F. Wong and T. Kurma, *Nanotechnology*, 2008, **19**, 345702.
8 A. Frey, M. R. Neutra and F. A. Robey, *Bioconjugate Chem.*, 1997, **8**, 424–433.
9 K. Savolainen, H. Alenius, H. Norppa, L. Pylkkänen, T. Tuomi and G. Kasper, *Toxicology*, 2010, **269**, 92–104.
10 R. Shrivastava, S. Raza, A. Yadav, P. Kushwaha and S. J. Flora, *Drug. Chem. Toxicol.*, 2014, **37**, 336–347.

11 Q. L. Zhang, M. Q. Li, J. W. Ji, F. P. Gao, R. Bai, C. Y. Chen, Z. W. Wang, C. Zhang and Q. Niu, *Int. J. Immunopathol. Pharmacol.*, 2011, **24**, 23S–29S.
12 Q. Zhang, L. Xu, J. Wang, E. Sabbioni, L. Piao, G. M. Di and Q. Niu, *J. Biol. Regul. Homeost. Agents.*, 2013, **27**, 365–375.
13 L. Xu, Q. L. Zhang, F. P. Gao, J. S. Nie and Q. Niu, *Zhonghua Yu Fang Yi Xue Za Zhi,* 2010, **44**, 785–789.
14 J. W. Ji, Q. L. Zhang, R. Bai, F. P. Gao, C. C Ge, Z. W. Wang, C. Y. Chen, C. Zhang and Q. Niu, *Zhonghua Lao Dong Wei Sheng Zhi Ye Bing Za Zhi*, 2011, **29**, 434–436.
15 Y. Ding, L. N. Jia, B. Yang, G. Zhang, H. Y. Wang, W. W. Guo, X. F. Jia, C. C. Ge, Q. L. Zhang and Q. Niu, *Zhonghua Lao Dong Wei Sheng Zhi Ye Bing Za Zhi,* 2013, **31**, 744–748.
16 H. Kaminski, M. Beyer, H. Fissan, C. Asbach and T. A. J. Kuhlbusch, *Aerosol. Air. Qual. Res.*, 2014, **3**, 1–13.
17 M. Methner, L. Hodson, A. Dames and C. Geraci, *J. Occup. Environ. Hyg.,* 2010, **7**, 163–176.
18 S. J. Tsai, A. Ashter, E. Ada, J. L. Mead, C. F. Barry and M. J. Ellenbecker, *Nano*, 2008 (a), **3**, 301–309.
19 S. J. Tsai, A. Ashter, E. Ada, J. L. Mead, C. F. Barry and M. J. Ellenbecker, *Aerosol. Air. Qual. Res.*, 2008 (b), **8**, 160–177.
20 S. J. Tsai, E. Ada, J. A. Isaacs and M. J. Ellenbecker, *J. Nanopar.t Res.*, 2009, **11**, 147–161.
21 S. J. Tsai, R. F. Huang and M. J. Ellenbecker, *Ann. Occup. Hyg.*, 2010, **54**, 78–87.
22 E. Demou, W. J. Stark and S. Hellweg, *Ann. Occup. Hyg*., 2009, **53**, 829–838.
23 Y. H. Cheng, Y. C. Chao, C. H. Wu, C J. Tsai, S. N. Uang and T. S. Shih, *J. Hazard. Mater.*, 2008, **158**, 124–130.
24 D. Brouwer, *Toxicology*, 2010, **269**, 120–127.
25 Y. Fujitani, T. Kobayashi, K. Arashidani, N. Kunugita and K. Suemura, *J. Occup. Environ. Hyg*., 2008, **5**, 380–389.
26 D. Bello, A. J. Hart, K. Ahn, M. Hallock, N. Yamamoto, E. J. Garcia, M. J. Ellenbecker and B. L. Wardle, *Carbon*, 2008, **46**, 974–981.
27 E. Demou, P. Peter, and S. Hellweg, *Ann. Occup. Hyg.*, 2008, **52**, 695–706.
28 M. M. Methner, *Int. J. Occup. Env. Heal.*, 2010, **16**, 475–487.
29 J. Y. Park, G. Ramachandran,P. C. Raynor, L. E. Eberly and G. O. Jr, *Ann. Occup. Hyg.,* 2010, **54**, 799-812.
30 K. Hameri, I. K. Koponen, P. P. Aalto and M. Kulmala, *J. Aerosol. Sci.,* 2002, **33**, 1463–1469.
31 M. B. Zhang, L. Jian, P. F. Bin, M. L. Xing, J. L. Lou, L. M. Cong and H. Zou, *J. Nanopart. Res.*, DOI 10.1007/s11051-013-2016-4.
32 A. Keller, M. Fierz, K. Siegmann, H. C. Siegmann and A. Filippov, *J. Vac. Sci. Technol.,* 2001, **19**,1–8.
33 W. A. Heitbrink, D. E. Evans, B. K. Ku, A. D. Maynard, T. J. Slavin and T. M. Peters, *J. Occup. Environ. Hyg.*, 2009, **6**, 19–31.
34 L. Morawska, H. Wang, Z. Ristovski, E. R. Jayaratne, G. Johnson, H. C. Cheung, X. Ling and C. He, J Environ Monit., 2009, **11**, 1758–1773.
35 OECD, OECD working party for manufactured nanomaterials (WPMN), ENV/JM/MONO. 2009, **11**, 16.
36 G. Ramachandran, D. Paulsen, W. Watts and D. Kittelson, *J. Environ. Monit.*, 2005, **7**, 728–735.
37 W. A. Heitbrink, D. E. Evans, B. K. Ku, A. D. Maynard, T. J. Slavin and T. M. Peters, *J. Occup. Environ. Hyg.*, 2009, **6**,19–31.
38 A. D. Maynard and R. J. Aitken, *Nanotoxicology*, 2007, **1**, 26–41.
39 A. D. Maynard, P. A. Baron, M. Foley, A. A. Shvedova, E. R. Kisin and V. Castranova, *J. Toxicol. Env. Heal. A*, 2004, **67**, 87–107.
40 B. Yeganeh, C. M. Kull, M. S. Hull and L. C. Marr, *Environ. Sci. Technol.*, 2008, **42**, 4600–4606.
41 X. Y. Li, P. S. Gilmour, K. Donaldson and W. MacNee, *Thorax*, 1996, **51**, 1216–1222.
42 V. Stone, J. Shaw, D. M. Brown, W. Macnee, S. P. Faux and K. Donaldson, *Toxicol. In Vitro,* 1998, **12**, 649–659.
43 G. Oberdörster, *Phil. Trans. R. Soc. Lond. A.*, 2000, **358**, 2719–2740.
44 C. L. Tran, D. Buchanan, R. T. Cullen, A. Searl, A. D. Jones and K. Donaldson, *Inhal. Toxicol.,* 2000, **12**, 1113–1126.
45 D. M. Brown, M. R. Wilson, W. MacNee, W. Stone and W. Donaldson, *Toxicol. Appl. Pharmacol.*, 2001, **175**, 191–199.
46 T. Stoeger, C. Reinhard, S. Takenaka, A. Schroeppel, E. Karg, B. Ritter, J. Heyder and H. Schulz, *Environ. Health. Perspect.*, 2006, **114**, 328–333.

Table 1 General information on the sampling locations

Sampling site	Reason for particle release	Engineering control	Sampling day [a]	Timeline of test protocol
Separation (unstable status)	Excessive air pressure for back-flushing in separator led to considerable release of particles from a cold-air inlet	General ventilation	Day 1	13:27~15:45
Outdoor background	-	-	Day 1	16:20~17:20
Packaging	Automatic packaging of powder in the semi-open process	Dust extraction device	Day 2	8:38~11:38
Separation (stable status)	High pressure for air back-flushing in separator led to particle release from a cold-air inlet	General ventilation	Day 2	14:20~16:21
Outdoor background	-	-	Day 2	16:35~17:35

[a]: Day 1 was a typical day during which the production status was sometimes unstable in the trial phase of production; Day 2 was a representative among the three-day sampling period during which the production status and working condition kept stable.

Table 2 Monitoring and sampling system for measuring Al_2O_3 nanoparticles

Monitoring types	Exposure metrics	Instruments	Particle sizes	Measuring range	Sampling rate	log interval
Real-time monitoring	Respirable MC	DustTrak 8530 (TSI, USA)	100~1000 nm	0.001~150 mg/m^3	3 L/min	1 min
	Total NC	P-Trak 8525 (TSI, USA)	20~1000 nm	0~500,000 particles/cm^3	0.1 L/min	1 min
	Size distribution by number	SMPS 3034 (TSI, USA)	10~487 nm	1~2.4×10^6 particles/cm^3	1.0 L /min	3 min
	Active SAC	Aero TrakTM 9000 (TSI, USA)	10~1000 nm	1~10000 μm^2 /cm^3	2.5 L/min	1 min
Membrane-based sampling	Size distribution by mass	Nano-MOUDI 125A (MSP, USA); Aluminium foil	10~10000 nm	-	10.0 L /min	-
	Morphology	SEM S4800 (HITACHI, Japan)	10~10000 nm	-	-	-
	Elemental composition	EDX (HITACHI, Japan)	10~10000 nm	-	-	-

MC: mass concentration; NC: number concentration; SAC: surface area concentration; SEM: scanning electron microscopy; EDX: energy-dispersive X-ray spectroscopy.

Table 3 Characteristics of Al_2O_3 nanoparticles at separation and packaging locations

Metrics	Separation (unstable)		Separation (stable)		Packaging		Indoor transportation		Background
	(median, range)	CR	(mean ± SD)	CR	mean ± SD	CR	(mean ± SD)	CR	(mean ± SD)
$NC_{20–1000nm}$ ($10^5/cm^3$)	0.94 (0.26–4.96) [ab]	4.94	0.43 ± 0.11 [a]	2.26	0.34 ± 0.07 [a]	1.79	0.56± 0.09 [a]	2.95	0.19 ± 0.02
Respirable $MC_{100–1000nm}$ (mg/m^3)	0.64 (0.10–11.80) [ab]	12.8	0.20 ± 0.14 [a]	4	0.46 ± 0.17 [a]	9.2	0.51 ± 0.11 [a]	10.20	0.05 ± 0.01
Active $SAC_{10–1000nm}$ ($\mu m^2/cm^3$)	110.37 (46.16–1567.30) [ab]	6.15	76.61 ± 26.86 [a]	4.27	56.54 ± 24.08 [a]	3.15	92.70 ± 10.99 [a]	5.16	17.95 ± 0.95
Estimated $SAC_{10–487nm}$ ($\mu m^2/cm^3$)	8261.59 (1333.94–27795.30) [abc]	15.52	3341.38 ± 2531.68 [ac]	6.28	1352.78 ± 135.20 [ac]	2.54	3194.32± 480.82 [ac]	6.00	532.37 ± 42.32 [c]
Shape	Bimodal or irregular	-	Bimodal	-	Bimodal	-	Bimodal		Unimodal
Mode size (nm)	34.00 (21.29–305.05)	-	-	-	-	-	-	-	20.37 ± 4.56
First peak	-	-	305.05 ± 0.01	-	90.09 ± 33.40	-	99.70 ± 9.46	-	-
Second peak	-	-	26.11± 3.51	-	26.58 ± 5.13	-	23.11 ± 1.64	-	-
APN of nanoparticles (%)	61.55 (44.88~85.08)	-	43.53 ± 4.45	-	73.27 ± 0.54	-	-	-	90.39 ± 0.68
APM of nanoparticles (%)	24.87	-	20.00	-	21.62	-	-	-	25.00

NC: number concentration; MC: mass concentration; SAC: surface area concentration; APN: accumulative percentage by number, among total particles ranged from 10 to 469.8 nm; APM: accumulative percentage by mass, among total particles ranged from 10 to 560 nm. [a]: $p<0.01$, as compared with outdoor background; [b]: $p<0.01$, as compared with stable production status; [c]: $p<0.01$, as compared with active SAC.

Table 4 Chemical compositions of sampled nanoparticles and outdoor background particles

Sampling location	Constituent elements (% by mass)
Outdoor	C (70.13), O (26.89), Na (0.87), Si (0.75), S (0.17), Fe (1.18)
Packaging	C (13.71), O (38.20), Al (46.03.91), Si (0.81), Cl (1.26)
Separation (unstable production)	C (18.60), O (49.12), Al (27.48), Si(1.24), Cl (2.42), Fe (0.58), Zn(0.56)
Separation (stable production)	C (14.39), O (28.39), Al (52.64), Si (1.69), Cl (0.92), Na(0.52), Ca(0.72), Fe(0.73)

Table 5 Key events associated with significant changes in particle concentrations

Sampling site	Figure	Sampling date	Time	Key event
Separation	Fig 3 (a)	Day 1	13:30–14:27	Particle spraying from a cold-air inlet of separator due to frequent air back-flushing at excessive pressure
	Fig 6 (a)	Day 2	15:11–16:20	Greatly increased particle leakage from a cold-air inlet
	Fig 3(b)	Day 2	14:53	Particle spraying from a cold-air inlet
		Day 2	15:26	Particle spraying from a cold-air inlet
Packaging	Fig 5 (a) Fig 5 (b) Fig.6 (b)	Day 2	9:44–9:50	A liquid nitrogen container was transported past the sampling location and a nearby workshop door was opened, leading to re-entrainment of dust from the floor
		Day 2	10:26–10:29	The door of the packaging device was opened to collect the end-product
		Day 2	11:12–11:15	The door of the packaging device was again opened to collect the end-product

Table 6 Correlations between mass-, number- and surface concentrations for all samples (n=878)

Variables	Respirable $MC_{100–1000nm}$	$NC_{20–1000nm}$	Active $SAC_{10–1000nm}$
Respirable $MC_{100–1000nm}$ (mg/m^3)	1.000	-	-
$NC_{20–1000nm}$ ($10^5/cm^3$)	0.361[a]	1.000	-
Active $SAC_{10–1000nm}$ ($\mu m^2/cm^3$)	0.666[a]	0.823[a]	1.000

NC: number concentration; MC: mass concentration; SAC: surface area concentration

[a] $p<0.01$

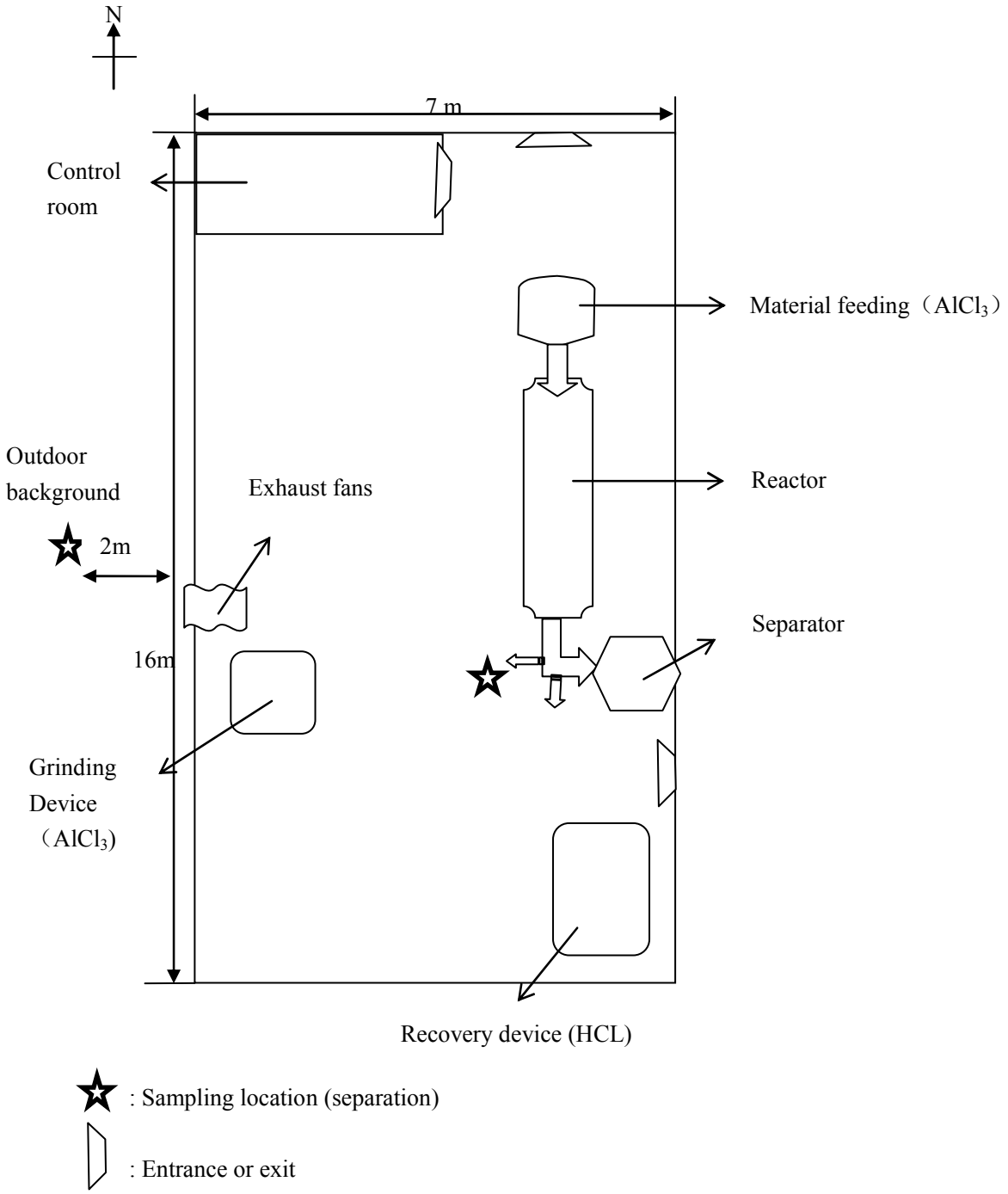

Fig.1 (a) Production workshop layout and sampling location

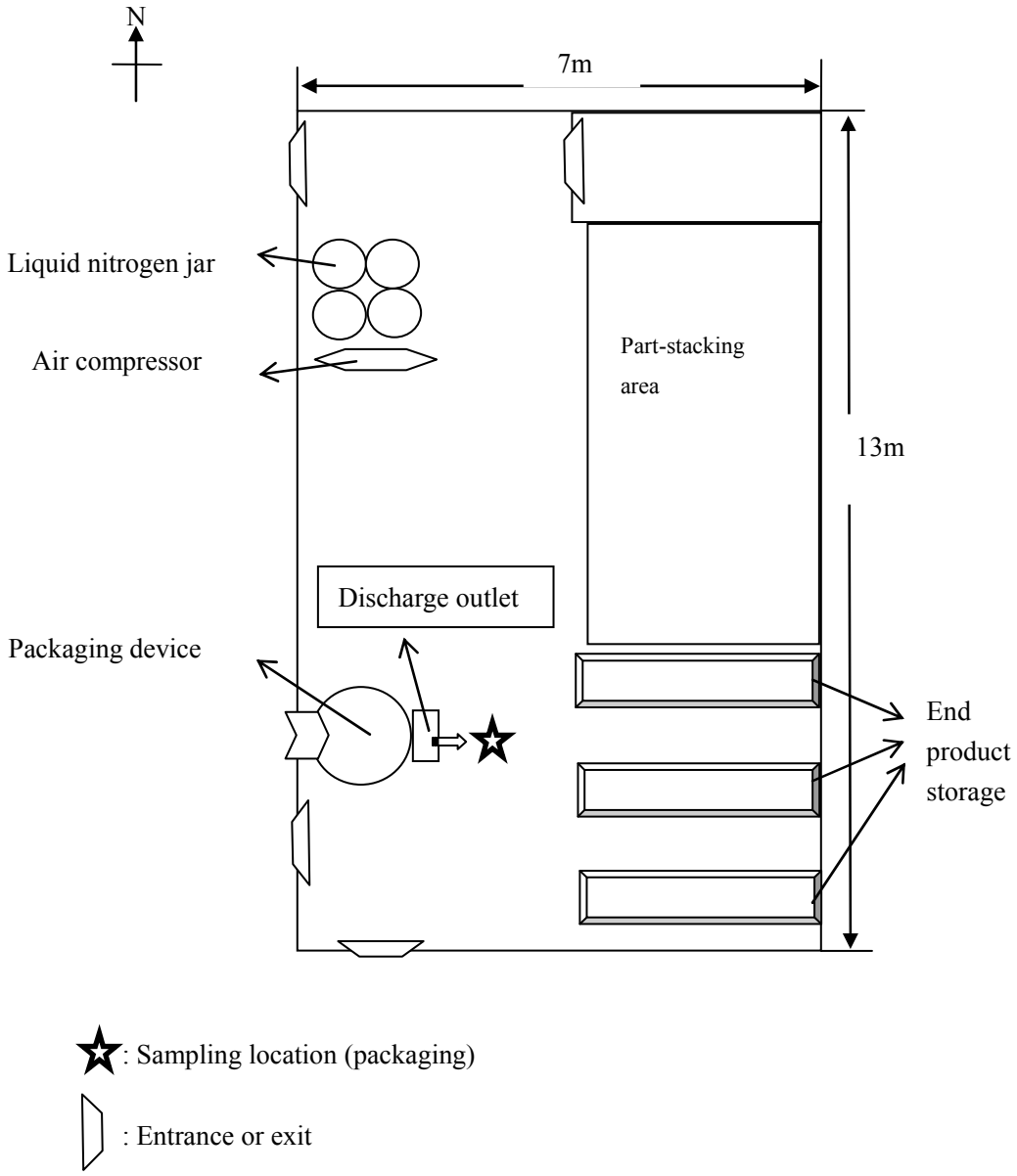

Fig.1 (b) Packaging workshop layout and sampling location

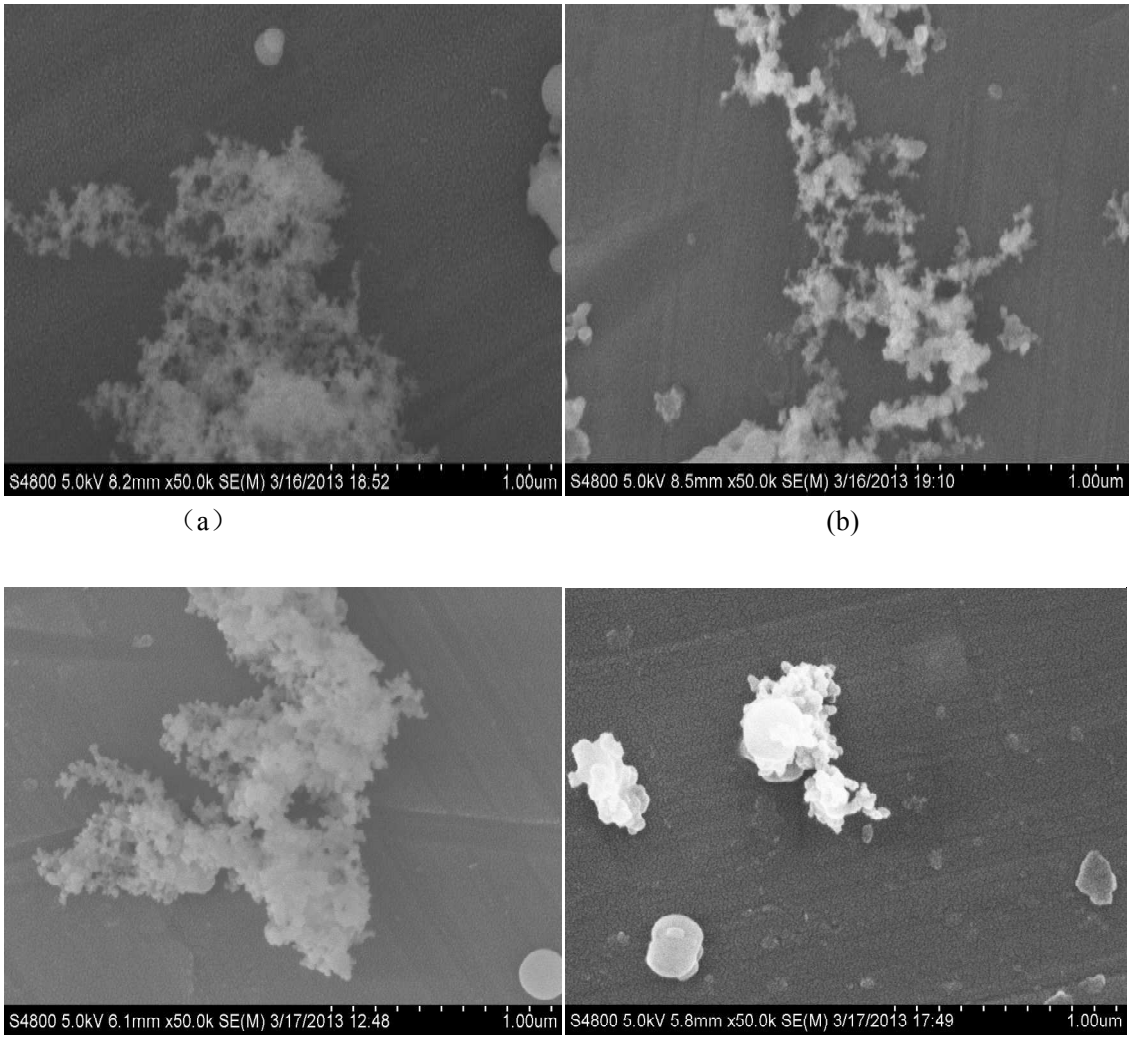

（a） (b)

(c) (d)

Fig. 2 Scanning electron micrographs of the Al_2O_3 nanoparticles and the background particles: (a) floccus agglomerates of Al_2O_3 nanoparticles collected at a cold air inlet of separation device under the unstable production status; (b) floccus agglomerates of Al_2O_3 nanoparticles collected at a cold air inlet of separation device under the stable production status; (c) cloud-like agglomerates of Al_2O_3 nanoparticles collected at a packaging location; (d) irregular outdoor-background particles.

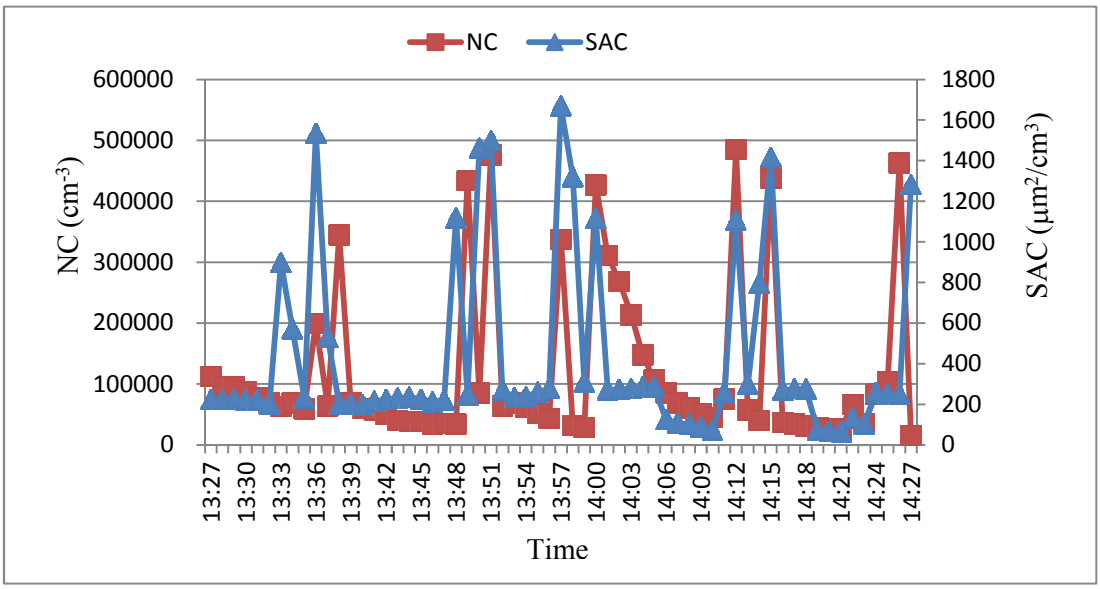

(a)

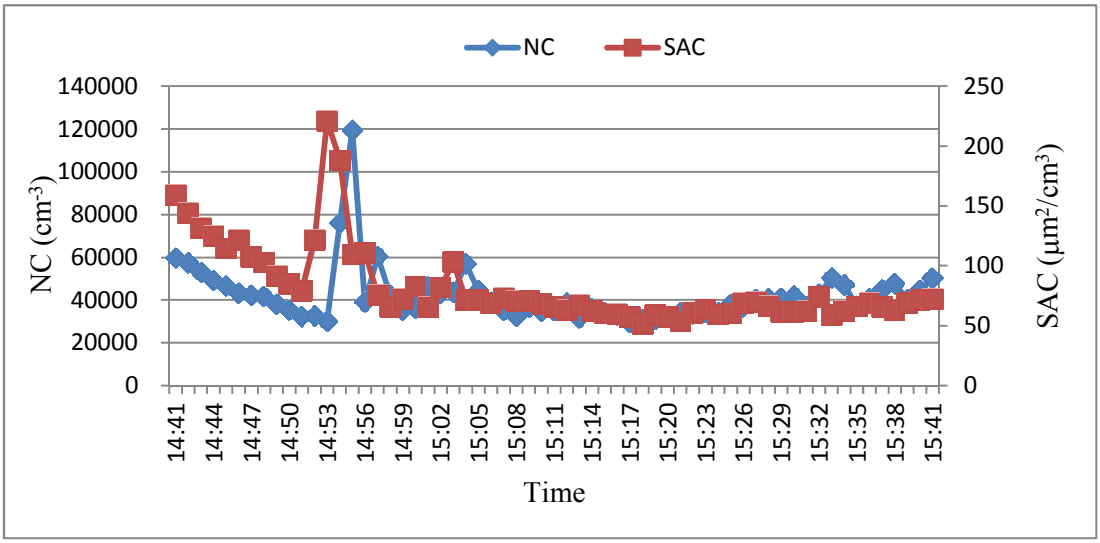

(b)

Fig.3 Temporal variations in number concentration (NC) and surface concentration (SAC) at the separation location: (a) unstable production status; (b) stable production status.

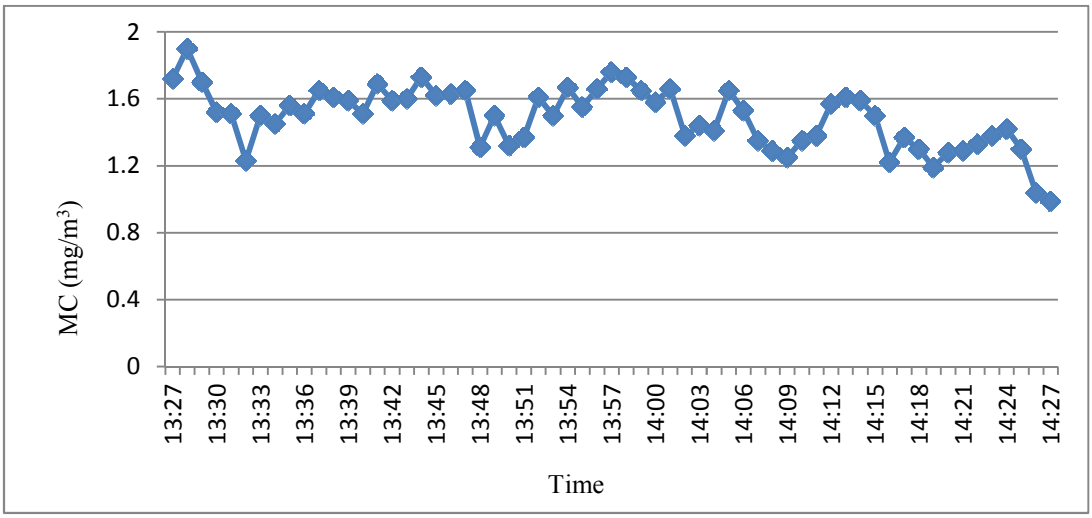

(a)

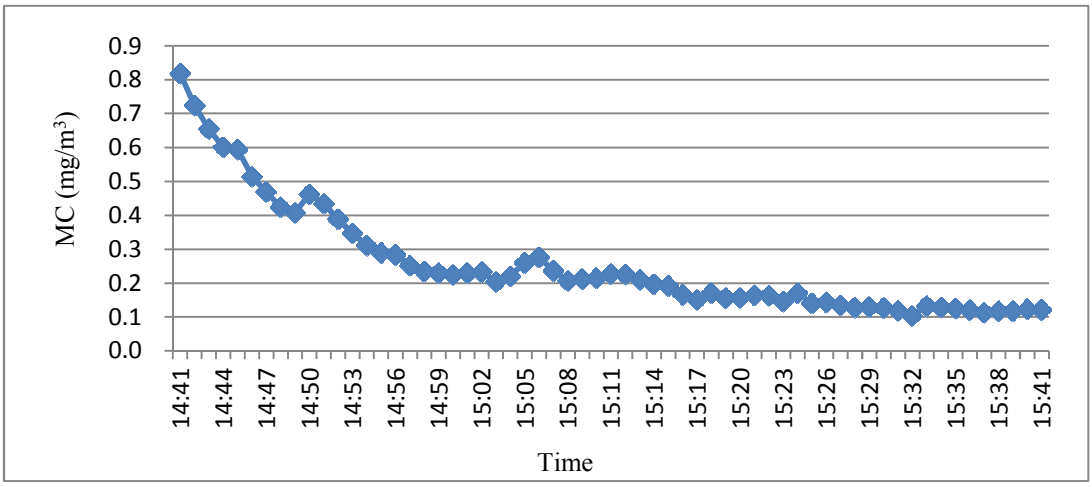

(b)

Fig.4 Temporal variations in mass concentration (MC) at the separation location: (a) unstable production status; (b) stable production status.

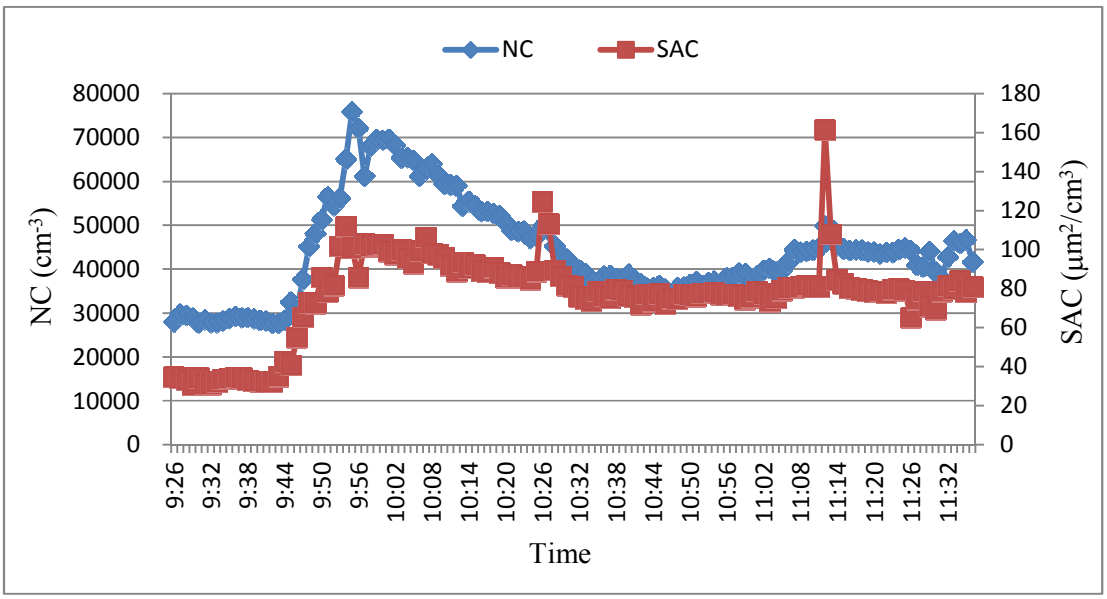

(a)

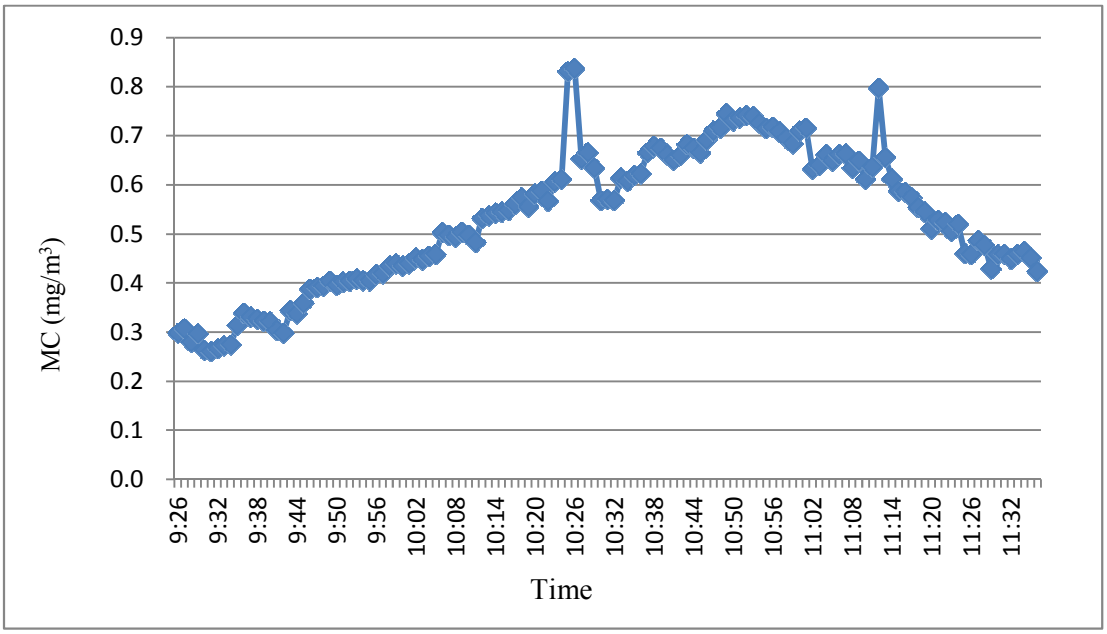

(b)

Fig.5 Temporal variations in total particle concentration at the packaging location: (a) number concentration (NC) and surface area concentration (SAC); (b) mass concentration (MC).

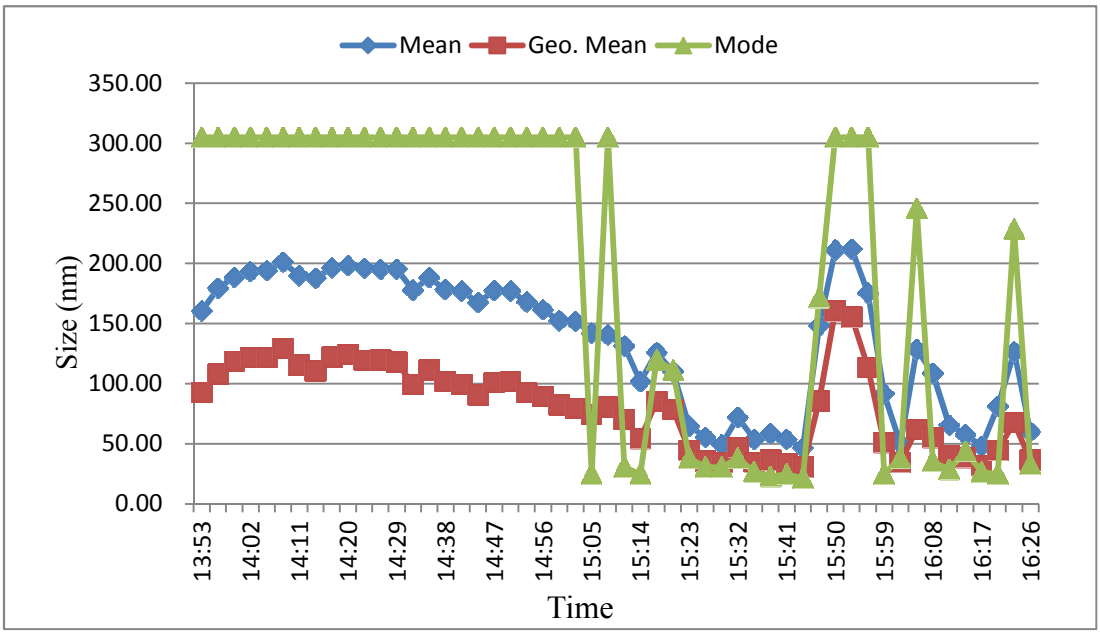

(a)

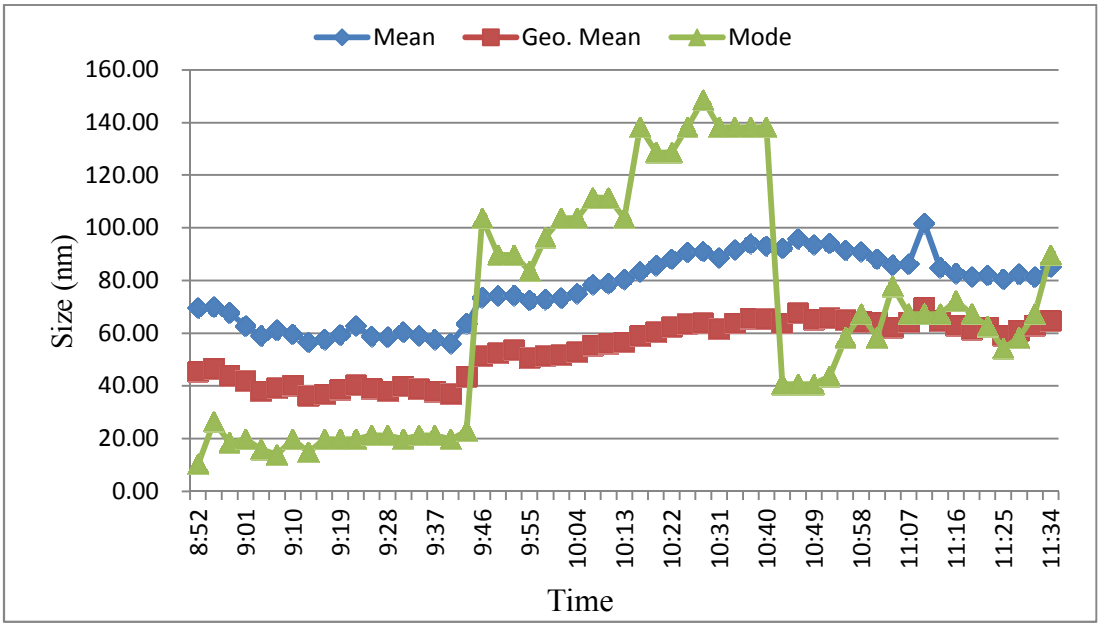

(b)

Fig.6 Temporal variations in mode, arithmetic mean and geometric mean particle sizes: (a) separation; (b) packaging.